RSC Advances

ROYAL SOCIETY OF CHEMISTRY

www.rsc.org/advances

Journal Name

ARTICLE

High contrast off-on fluorescence photo-switching *via* copper ion recognition, *trans-cis* isomerization and ring closure of a thiosemicarbazide Schiff base

Received 00th January 20xx,
Accepted 00th January 20xx

DOI: 10.1039/x0xx00000x

www.rsc.org/

Wei Li[a], Xiaoping Gan[a, b], Dan Liu[a], Xiaohe Tian[a], Jianhua Yu[a], Yupeng Tian[a], Jieying Wu[a], Hongping Zhou[a,*]

An easily available triphenylamine-isophorone-based Schiff base was synthesized and its specifically triple-addressable molecular photo-switching behaviour *via* copper ion recognition, *trans-cis* isomerization and ring closure were investigated in detail. Firstly, compound Lo was able to real-time monitor Cu^{2+} in acetonitrile solution via displaying the "turn-on" emission in the near infrared region with high selectivity, sensitivity. Furthermore, two independently photochromic phenomena based on the distinct mechanisms were found surprisingly, one through the ring closure of thiosemicarbazide moiety based on Michael addition reaction in tetrahydrofuran solution and another through the *trans-cis* isomerization of aldimine (–C=N–) in solid state under the stimuli of UV/Visible light. Finally, fluorescence imaging experiments in living cells demonstrated the potential practical applications in biological systems.

Introduction

As the third most abundant (after Fe^{3+} and Zn^{2+}) essential metal ion in the human body, Cu^{2+} ion plays a pivotal role in various fundamental physiological processes[1]. However, overloaded levels of Cu^{2+} can cause oxidative stress and disorders associated with neurodegenerative diseases, and Cu^{2+} ion is also identified as an environmental pollutant, which is potentially very toxic to organisms[2]. Consequently, the development of high-performance fluorescent probes for the determination and visualization of Cu^{2+} ion has been received considerable attention because of high selectivity, sensitivity, specificity, low detection limit and real-time monitoring with fast response[3].

Photochromic molecules are better known by the possibility of achieving reversible changes in the color upon light absorption. Moreover, they may also find many other applications such as switches[4], optical memory devices[5], sensors[6], or holographic gratings[7]. Two main mechanisms to achieve photochromism are the *cis-trans* isomerization and the opening-closure ring, azobenzenes[8] or stilbenes[9] and diarylethenes[10] or spiropyrans[11], respectively, often reported in literature. However, instances of turn-on fluorescence of other photochromic systems upon irradiation with UV/Visible light are rather rare. In a previous work[12], we reported that a triphenylamine Schiff base having the diaminomaleonitrile unit exhibited highly sensitivity and selectivity for Cu^{2+} ion by the ring-closing of diaminomaleonitrile moiety based on Michael addition reaction and coordination interaction. Malkondu reported[13] a novel triphenylamine based semicarbazone Schiff base TOC, and exhibited fluormetric 'turn-on' response towards Cu^{2+} *via* a unique cyclization reaction. The preliminary work have contributed to expanding the kinds of photochromic molecular and further help us to understand their photochromic mechanisms.

In this communication, a new thiosemicarbazide based photochromic Schiff base Lo was successfully synthesized and its specifically dual-addressable molecular photo-switching behaviour of interacting with Cu^{2+} ion and light (UV/Visible) were investigated in detail. The results will be helpful for synthesizing the efficient photoactive thiosemicarbazide derivatives with multi-addressable states and understanding the information processing on the unimolecular platform with potential applications in fluorescent chemosensors, data manipulation, as well as intelligent diagnostics.

Results and discussion

The Schiff base compound **Lo** was synthesized by aldol condensation and affinity addition-elimination reaction. The synthetic details are presented in **Scheme 1**. The intermediate 0 reacted with intermediate 1, and underwent a classical aldol condensation to form intermediate 2. Furthermore, a simple condensation of the intermediate 2 with compound b in anhydrous methanol gave a Schiff base **Lo**. They were

[a]*College of Chemistry and Chemical Engineering, Anhui University and Key Laboratory of Functional Inorganic Materials Chemistry of Anhui Province, Hefei 230601, P. R. China.*
[b]*School of Science, Anhui Agricultural University, 230036 Hefei, P. R. China.*
[c]*Center of Stem cell Research and Transformation Medicine, Anhui University, Hefei 230601, P. R. China.*
[*]*Corresponding author. Fax: +86-551-63828106, Tel: +86-551-63828150.*
E-mail address: zhpzhp@263.net
†Electronic Supplementary Information (ESI) available: Synthesis, characterization spectra and theoretical calculations. See DOI:10.1039/b000000x/

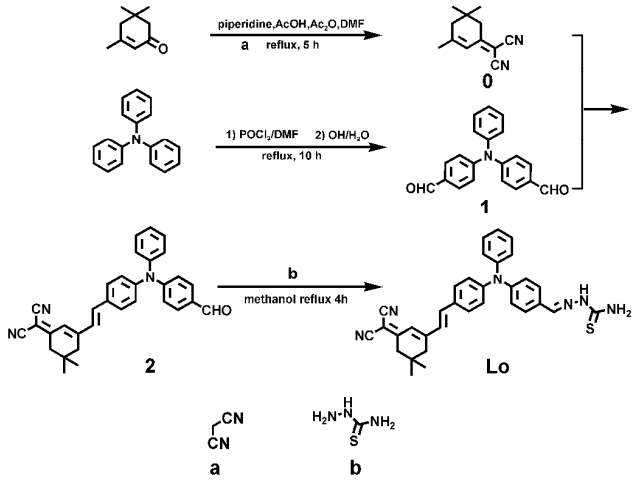

Scheme 1. Synthesis route of compound **Lo**

characterized by ^{1}H NMR, ^{13}C NMR spectrum, mass spectrum, FT-IR and elemental analysis. For **Lo**, the presence of a singlet at 8.16 ppm corresponds to the aldimine proton (−HC=N−), which is further testified by 1687 cm^{-1} in IR spectrum. The singlet at 8.01 ppm corresponds to the amido ($-NH_2$), which is tested by 3413 cm^{-1} in IR spectrum. The singlet at 7.62 ppm stands for $-H_2C=CH_2-$ proton, which is obtained at 831 cm^{-1} in the IR spectrum.

The compound **Lo** was soluble in acetone, acetonitrile, DMF and DMSO, tetrahydrofuran, dichloromethane and chloroform. It was partially soluble in water, methanol, ethanol. The photo/solution stability of compound **Lo** was thus monitored by UV-visible spectroscopy in acetonitrile (under visible light) and tetrahydrofuran (under dark light). And the absorption spectral of compound **Lo** shows no apparent spectral change even after 72 hours (**Fig. S1, ESI†**).

Recognition ability toward metal ions

With that, we evaluated its spectral properties in the presence of some environmentally or physiologically important metal ions in the CH_3CN solution. As shown in **Fig. 1a**, Cu^{2+} ion induced significant change in the emission spectra, whereas no distinct change was observed upon the addition of other ions. Consistent with the fluorescent enhancement, an apparent color change from dull-red to bright-red was observed by naked-eye under a UV lamp of 365 nm (**Fig.1a inset**). Also, the fluorescence enhancement upon addition of Cu^{2+} ion almost remained unchanged even after adding large amounts of other competitive metal ions (**Fig. S2, ESI†**).This result indicated the high selectivity of probe **Lo** for Cu^{2+} over other competitive metal ions in acetonitrile solution. As evident from **Fig.1b**, the fluorescence emission centred at 631 nm gradually increased along with the increasing amount of Cu^{2+} and when the concentration of Cu^{2+} ions reached 2.0 equivalent, a maximal fluorescence enhancement (31-fold) was observed. This fluorescence enhancement in the NIR region is superior to the known fluorescent Cu^{2+} probes with emission only in the

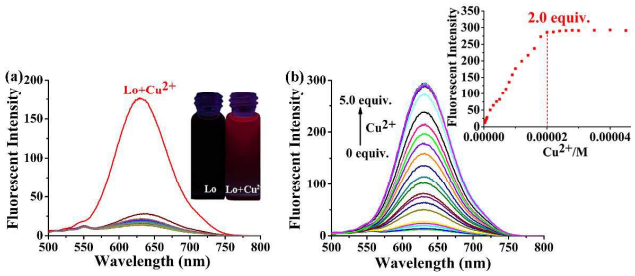

Fig. 1 (a) Fluorescence spectra of **Lo** (10 μM) in CH_3CN in the absence and presence of different metal ions (10 μM). Inset: color of Lo and **Lo** + Cu^{2+} system under UV lamp at 365 nm; (b) Fluorescence spectra of **Lo** (10 μM) upon the addition of Cu^{2+} (0-5.0 equivalent.). Inset: fluorescence intensity changes at 631 nm of **Lo** (10 μM) with the equiv. of Cu^{2+} ions.

visible region. Obviously, the stoichiometry showed 1:2 for the **Lo**-Cu^{2+} complexation (**Fig.1b, inset**), which was further confirmed by Job plot analysis (**Fig. S3, ESI†**)[14]. Based on fluorescence titration data, the binding constant[15] of **Lo** with Cu^{2+} in acetonitrile (**Fig. S4a, ESI†**) was found to be 2.076×10^{4} M^{-1}. Fluorometric titration data was also used to obtain the detection limits of **Lo** for Cu^{2+}. The detection limits of **Lo** was found to be 4.275×10^{-7} M for Cu^{2+} (**Fig. S4b, ESI†**) based on the equation DL = K× SD/S, where K = 3, SD is the standard deviation of the blank solution, and S is the slope of the calibration curve[16-17], which is much lower than the limit of copper (~20 μM) in drinking water by the U.S. Environmental Protection Agency[18], indicating that it could quantify Cu^{2+} in lower than micromolar level. Further, the pH titration (**Fig. S5, ESI†**), the reversibility (**Fig. S6, ESI†**) and the response time experiment (**Fig. S7, ESI†**) were also carried out. All results demonstrated that **Lo** was able to real-time monitor Cu^{2+} *via* displaying the "turn-on" emission in the NIR region with high selectivity, sensitivity.

The favorable features of the probe **Lo** include emission in the NIR region, a significant fluorescence turn-on signal, high sensitivity, high selectivity, and functioning well at physiological pH. These desirable characters prompted us to evaluate the ability of the probe to image Cu^{2+} in living cells. As shown in **Fig. 2**, HepG2 cells treated with 10 μM of **Lo** exhibited the ignorable emission, however, once incubated with the solution of $Cu(NO_3)_2$ (100 μM) for 0.5 h, the whole cell

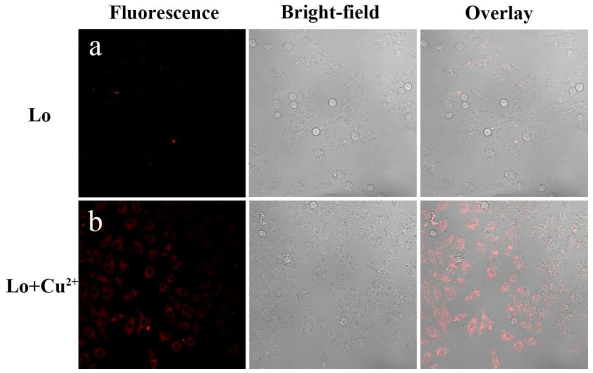

Fig.2 Fluorescence microscopy of HepG2 cells for (a) cells treated with 10 μM of **Lo**; (b) treated with 100 μM of Cu^{2+} to (a).

displayed remarkable fluorescence enhancement in the cell cytoplasm areas. At the same time, to evaluate cytotoxicity of the probe, **Lo** was taken as an example to perform a 3-(4,5-dimethylthiazol-2-yl)-2,5-diphenyltetrazolium bromide (MTT) assay on HepG2 cells with the concentration from 0 μM to 40 μM. The cellular viability estimated was ca. 91.2% in 24 h after treatment with 40 μM of **Lo**, exhibiting low toxicity to cultured cells (**Fig. S8, ESI†**). Furthermore, good photostability of **Lo** was also evaluated by photon-bleach experiment (**Fig. S9, ESI†**). These data indicate that the probe **Lo** can penetrate the cell membrane and sense exogenous Cu^{2+} in the living cells effectively in a non-invasiveness way, with the switching-on fluorescent signal.

Photochromic reaction

Photochromic reaction under solution

Unexpectedly, the photochromic behavior of compound **Lo** in THF and the others solvents (**Fig. S10, Table S1, ESI†**) at room temperature was discovered. Immediately following this find, the ring closure photochromic process from **Lo** (open-ring isomer) to **Lc** (closed-ring isomer) after irradiation with visible light was demonstrated by ^{1}H NMR[19]. As illustrated in **Fig. 3**, as the growth of the irradiation time, the signals of aldimine protons (Hb) and amidogen protons (Ha) gradually disappeared. Meanwhile, the new signal assignable to para amide (Hc) appeared at 2.280 ppm became more and more obvious. Moreover, by comparing the MALDI-TOF mass spectrometry (**Fig. S11, ESI†**), we found that the original peak at m/z 542.227 for free **Lo** disappeared and a new peak at m/z 540.202 for the corresponding closed-ring compound **Lc** emerged after irradiation with visible light. Overall results indicated that **Lo** underwent a closure-ring process after irradiation with visible light. Furthermore, we began to research their ultraviolet and fluorescence spectral properties. **In Fig. 4**, UV-visible

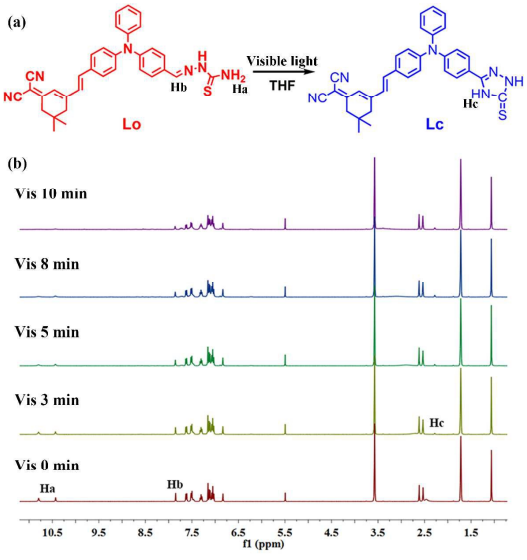

Fig. 3 (a) Changes in chemical structure of **Lo** under the alternative irradiation with visible light in THF; (b) Changes in ^{1}H NMR spectrum of **Lo** under the alternative irradiation with visible light in THF.

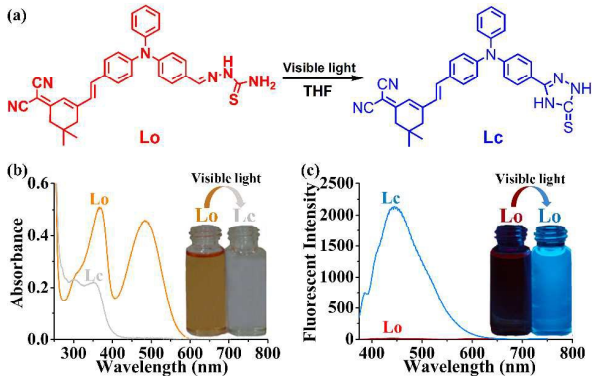

Fig. 4 (a) Changes in chemical structure of **Lo** under the alternative irradiation with visible light in THF; Absorption (b) and Fluorescent (c) spectra of **Lo** in THF solution before and after visible irradiation.

spectrum of **Lo** (10 μM) displayed absorption bands at 484, 368 nm, under visible light irradiation (10 min, 100 μM), this orange solution turned to colorless and the absorption of the open-ring isomer at a shorter wavelength (368 nm) decreased gradually while a longer wavelength (484 nm) vanished, eventually formed the closed-ring isomer. Meanwhile, the original fluorescent band at 620 nm (red color) disappeared and a new band centred on 431 nm (blue color) was observed and its intensity increased with the increasing of irradiation time (**Fig. S12, ESI†**). Furthermore, compared with **Lo**, **Lc** displayed 36-fold higher quantum yields and fluorescence lifetimes (**Fig. S13, Table S2, ESI†**).

The above described properties inspired us to investigate photochromism in living cells. Herein, live cells treated with the opening form of compound **Lo** initially showed a red fluorescence signal, but after 30 min of visible light irradiation, a substantial cytoplasmic blue fluorescence signal appeared, suggesting a conversion of **Lo** into the closed-form isomer **Lc** in vitro, as shown in **Fig. 5**.

In order to explored the cell viability after long photo-exposure time (**Fig. S14, ESI†**). One reliable way to assess the in-vitro anticancer activity of a compound is to evaluate its cytotoxicity in terms of its half maximal inhibitory concentration (IC_{50}) value in cancer cells by using the MTT (3-(4,5-dimethylthiazol-2-yl)-2,5-diphenyltetrazolium bromide) assay[20]. Therefore, the anticancer activity of the compound **Lo** was evaluated by the MTT assay in HepG2 cells in the

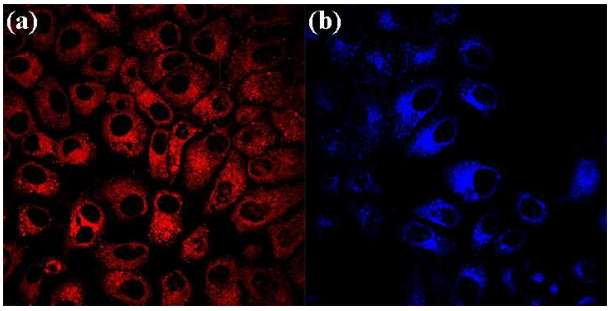

Fig. 5 (a) The confocal laser scanning microscope image of HepG2 cells incubated with **Lo** (100 μM) for 20 min at 25 °C (a) in original state, (b) irradiated by 405 nm light for 30 min.

presence of visible light (400-700 nm, 10 J cm^{-2}) for 0.5 h, giving IC_{50} values of 70 μM, and >105 μM in the absence of light, which indicated the compound Lo had not significant toxicity in HepG2 cells under visible light.

The dual-colour photochromic property of **Lo** make it an ideal tool for bioimaging applications with either red or blue fluorescence.

Photochromic reaction under solid

In the past decade, a number of photochromic molecules show photoisomerization under the solid state have been proposed. However, the most of those molecules in solid state showed the same photochromic mechanism as solution state. Based on the abnormal cyclization in aqueous solution and the characteristics of Schiff bases tend to occur *trans-cis* isomerization in solid state, the design and development of photochromic molecules with distinct photochromic mechanisms in solid and solution state is a wide topic.

Excitingly, the distinct color change of the **Lo** under solid state was observed when it was exposed to appropriate light (**Fig. 6a**). Using the selective 365 nm light irradiation through an aluminum mask, the exposed regions turned gradually to red with 22-fold fluorescent enhancement at 690 nm, whereas the masked areas maintained the initial color, at the same time, it displayed 28-fold enhancement in fluorescence lifetimes and quantum yields (**Fig. S15, Table S3, ESI†**). On visible light illumination, the above process underwent a reversible reaction to the initial color. The ^{13}C NMR result displayed that the chemical shift (–C=N–) happened to small change from 149.50 to 150.81 ppm and no changes for others (**Fig. S16, ESI†**), which exhibited this photoluminescence derived from the *trans-cis* isomerization[21]. To gain more insight into the photophysical properties of *trans-cis* isomerization, the time-dependent density functional theory (TD-DFT) (B3LYP/6-31G(d)) calculations was also studied in **Fig. 7**. The energy gaps between HOMO and LUMO are 2.88 eV (**Lo-*trans***) and 2.93 eV (**Lo-*cis***). The **Lo-*trans*** is associated with lower energy than **Lo-*cis*** by 0.05 eV. Furthermore, experimentally **Lo-*trans*** and **Lo-*cis*** absorb at 569 and 551 nm while the theoretical

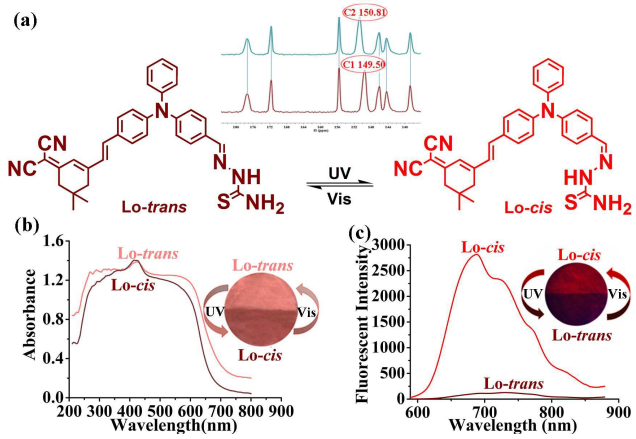

Fig. 6 (a) Changes in chemical structure under the alternative irradiation with UV and visible light in solid state; Absorption (b) and Fluorescent spectra (c) of **Lo-*trans*** in solid state before and after UV irradiation.

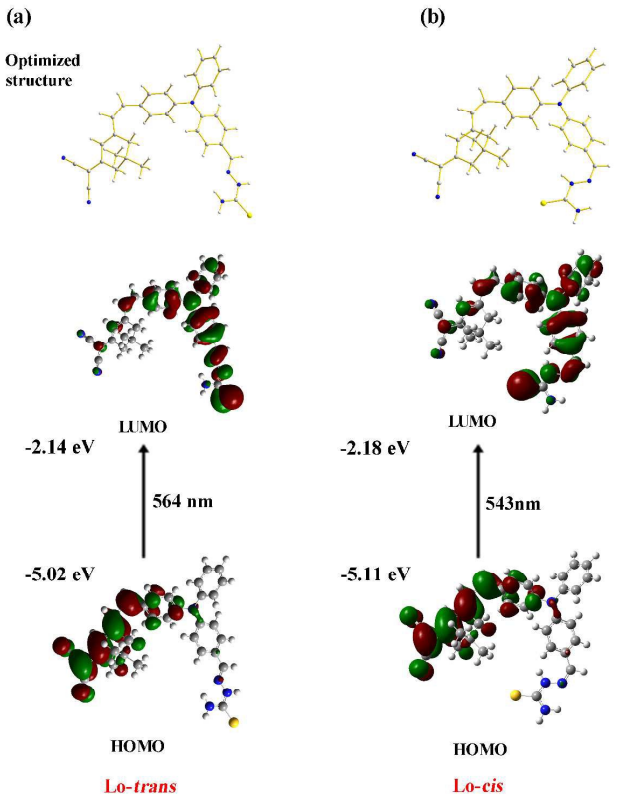

Fig. 7 Optimized geometries, HOMO and LUMO distributions of **Lo-*trans*** (a) and **Lo-*cis*** (b).

calculation showed absorption maxima at λ_{max} 564 nm (f = 0.8633) and λ_{max} 543 nm (f = 0.7531), the calculated absorption peaks correlate very well with the experimental observed values, which also confirmed that the photochromic properties should originate from the **Lo-*trans*** to **Lo-*cis*** isomeric reaction from experimental one. At the same time, The corresponding DFT coordinates for the optimized structures of **Lo-*cis*** and **Lo-*trans*** were also put in **Table S4-5** (**ESI†**). The delightful photoluminescence properties of the target compound might be utilized for practical development of solid-state photonic materials and photo-switchable accessories.

Conclusion

In conclusion, as far as we know this is the first clear demonstration of thiosemicarbazide based Schiff base about photochromic behaviours with distinctive color changes in response to distinguish mechanisms, which happened to the ring closure in THF solution and *trans-cis* isomerization in solid state under the stimuli of UV/Visible light. The dual photochromic compound is also showed excellent recognition ability toward Cu^{2+} in MeCN with high potential applications in sensing and labelling, as a consequence the system is able to respond to three stimuli. This example compared with many others reported literatures during the last few years shows the potentialities of this family of compounds, as versatile photochromic systems.

Experimental section

Materials and measurements

Unless otherwise mentioned, chemicals and solvents were purchased from commercially available resources and were used without further purification. ^{1}H NMR and ^{13}C NMR spectra were recorded on a Bruker AVANCE-400 MHz and 100 MHz, respectively and chemical shifts are expressed in ppm using TMS as an internal standard. The UV−vis absorption spectra were performed on a Shimadzu UV-265 spectrophotometer, and the fluorescence spectra were done using a Hitachi F-7000 fluorescence spectrophotometer with quartz cuvette (path length =1 cm). IR spectra were recorded with a Nicolet FT-IR NEXUS 870 spectrometer (KBr discs) in the 4000-400 cm-1 region. The mass spectrum were recorded by AXIMA-CFR plus MALDI-TOF MS. The elemental analysis was performed by Perkin Elmer 240B analyzer. The fluorescent life and quantum yield were performed on a HORIBA FluoroMax-4P full-function steady transient fluorescence spectrometer. The pH titration was carried out by using a METTLER TOLEDO FE20 pH meter.

The solutions of metal ions were prepared from $Pb(NO_3)_2$, $Co(NO_3)_2{\cdot}6H_2O$, $Zn(NO_3)_2{\cdot}6H_2O$, $Ca(NO_3)_2{\cdot}4H_2O$, $NaNO_3$, $LiNO_3$, $Cu(NO_3)_2{\cdot}3H_2O$, $Ni(NO_3)_2{\cdot}6H_2O$, $Bi(NO_3)_3{\cdot}5H_2O$, KNO_3, $Ba(NO_3)_2$, $Al(NO_3)_3{\cdot}9H_2O$, $Cd(NO_3)_2{\cdot}2H_2O$, $AgNO_3$, $Hg(NO_3)_2{\cdot}0.5H_2O$, $Cr(NO_3)_3{\cdot}9H_2O$, $Mg(NO_3)_2{\cdot}6H_2O$, $Fe(NO_3)_3{\cdot}9H_2O$ and $Mn(NO_3)_2{\cdot}4H_2O$.

Synthesis

Synthesis of compounds 0 and 1

Compounds **0** and **1** were prepared according to the literature[21].

Synthesis of compound 2

compound **0** (0.186 g, 1.0 mmol) and compound **1** (0.273 g, 1.0 mmol) were dissolved in acetonitrile (20 mL) under nitrogen. Piperidine (0.1 mL) was added as a catalyst and the mixture was reacted for 10 h at room temperature. The crude product was collected by filtration and purified by column chromatography (silica gel, petroleum ether/ethyl acetate= 25/1) to obtain red pure product. Yield: 60%. ^{1}H NMR (400 MHz, DMSO-*d*6) δ (ppm) (**Fig. S17, ESI†**): 9.82 (s, 1H), 7.79-7.77 (d, *J* = 8.2 Hz, 2H), 7.71-7.69 (d, *J* = 8.1 Hz, 2H), 7.73-7.46 (t, *J* = 7.4 Hz, 2H), 7.38-7.34 (d, *J* = 16.2 Hz, 1H), 7.30-7.25 (m, 2H), 7.20-7.19 (d, *J* = 7.8 Hz, 2H), 7.13-7.11 (d, *J* = 7.8 Hz, 2H), 7.03-7.01 (d, *J* = 8.2 Hz, 2H), 6.87 (s, 1H), 2.62 (s, 2H), 2.55 (s, 2H), 1.08-0.97 (s, 6H). ^{13}C NMR (100 MHz, $CDCl_3$) δ (ppm) (**Fig. S18, ESI†**):190.46, 169.13, 153.86, 152.57, 147.74, 145.78, 136.13, 131.42, 131.32, 130.26, 129.97, 128.86, 128.31, 126.64, 125.72, 124.90, 123.33, 122.14, 121.17, 78.31, 43.00, 39.24, 32.05, 28.04. MS (MALDI-TOF) (**Fig. S19, ESI†**): m/z 468.223 [(M-1)$^-$, calcd 468.215].

Synthesis of compound Lo

Thiosemicarbazide (0.0971 g, 1.066 mmol) and compound **2** (0.5 g, 1.066 mmol) were dissolved in anhydrous methanol (20 mL). Aceticacid (0.1 mL) was added as a catalyst and the mixture was refluxed for 2 h. Then the solution was concentrated to 10 mL and stood at room temperature for 3 h. The precipitate was filtered and washed 4 times with cold ethanol (20 mL). After drying under reduced pressure, dark red pure product was obtained (0.451 g). Yield: 73%. ^{1}H NMR (400 MHz, DMSO-*d*6) δ(ppm) (**Fig. S20, ESI†**):11.39 (s, 1H), 8.17 (s, 1H), 7.99 (s, 1H), 7.92 (s, 1H), 7.74-7.72 (d, *J* = 8 Hz, 2H), 7.64-7.62 (d, *J* = 8 Hz, 2H), 7.41-7.37 (t, *J* = 8 Hz, 2H), 7.32-7.23 (m, *J* = 16 Hz, 2H), 7.20-7.16 (d, *J* = 8 Hz, 2H), 7.13-7.11 (d, *J* = 8 Hz, 2H), 7.01-6.97 (t, *J* = 8 Hz, 2H), 6.83 (s, 1H), 2.61 (s, 2H), 2.54 (s, 2H), 1.02 (s, 6H). ^{13}C NMR (100 MHz, $CDCl_3$) δ (ppm) (**Fig. S21, ESI†**): 177.64, 170.20, 156.01, 148.06, 147.82, 145.13, 141.74, 137.41, 130.28, 130.23, 129.89, 129.32, 128.61, 127.79, 125.63, 124.77, 123.25, 122.54, 121.99, 114.03, 113.22, 75.29, 42.928, 38.22, 31.63, 27.41. FT-IR (KBr, cm−1) (**Fig. S22, ESI†**): 3413 (m), 3330 (m), 3276 (w), 3025 (w), 2951 (w), 2925 (w), 2869 (w), 2216 (s), 1594 (vs), 1559 (vs), 1522 (vs), 1496 (s), 1323 (m), 1278 (s), 1176 (m), 1154 (vs), 963 (m), 821 (w), 694 (w), 510 (w). MS (APCI) (**Fig. S23, ESI†**): m/z 542.227 [M, calcd 542.225]. EA：Calcd: C 73.03, N 15.49, H 5.57; Found: C 73.06, N 15.48, H 5.58.

Job plot

To determine the binding stoichiometry of the **Lo**-Cu^{2+} complex, Job plot is investigated by the fluorescence intensity of probe **Lo** at 637 nm were plotted as a function of their molar fraction under a constant total concentration (1×10^{-5} M), with a continuous variable molar fraction of Cu^{2+}.

Detection limits

The detection limit was determined by using fluorescence titrations. The fluorescence spectrum of **Lo** was measured 10 times and a standard deviation of a blank solution was achieved. To obtain the slope, the ratio of the fluorescence emission at 637 nm was plotted vs. the concentration of Cu^{2+} ions. The detection limit was calculated based on the equation DL = K× SD/S, where K = 3, SD is the standard deviation of the blank solution, and S is the slope of the calibration curve[22].

Effect of pH

Probe **Lo** (50 μL) was added in 4.95 mL acetonitrile–buffer solution (v/v = 9/1). The configuration of the buffer solution: pH 1-2, with HCl modulation directly; pH 3-4, with KHP/HCl modulation directly; pH 5-6, with KHP/NaOH modulation directly; pH 7-10, with HEPES/NaOH modulation directly; pH 11-13, with NaOH modulation directly. Here, the KHP is potassium hydrogen phthalate; 4-hydroxyethyl HEPES is piperazine ethyl sulfonic acid. All of the solution we had prepared act as solvent dilution.

Cell culture and imaging studies[23]

For HepG2 cells (liver hepatocellular carcinoma), the medium used was Dulbecco's Modified Eagle's Medium (DMEM) supplemented with 10% fetal calf serum (FCS, GIBCO), penicillin and streptomycin, L-glutamine and fungizone. For live cell confocal laser scanning microscopy experiment, HepG2 cells were seeded in 24-well glass bottom plate at density of 10,000, and incubated for 72-96 hours at 37 °C in 95% air 5% CO_2 in order to allow the cells to reach ~80% confluence, the medium changed every two days. Some of adherent cells were incubated with 10.0 μM probe **Lo** for 0.5 h at 37 ℃ under 5% CO_2 and then washed with PBS three times before incubating with 100.0 μM $Cu(NO_3)_2$ for another 0.5 h, cells were rinsed with PBS three times again, then the fluorescence imaging of intracellular Cu^{2+} was observed under a LSM710 confocal laser scanning microscope (Zeiss) with an objective lens (×60). The raw HepG2 cells only incubated with 10.0 μM **Lo** for 0.5 hour at 37 ℃ under 5% CO_2 was as a control.

Cytotoxicity assays in cells[24]

To ascertain the cytotoxic effect of the three compounds, the 3-(4,5-dimethylthiazol-2-yl)-2,5-diphenyltetrazolium bromide (MTT) assay was performed. HepG2 cells were trypsinized and plated to ~80% confluence in 96-well plates ($\sim 1\times10^4$ cells/well) 48 h before treatment. Prior to the compounds' treatment, the Dulbecco's Modified Eagle's Medium (DMEM) was removed and replaced with fresh DMEM, and aliquots of the compound stock solutions (1 mM DMSO) were added to obtain final concentrations of 5, 10, 20 and 40 μM. The treated cells were incubated for 24 h at 37℃and under 5% CO_2. Subsequently, the cells were treated with 5 mg / mL MTT (40 μL/well) and incubated for an additional 4 h (37 ℃, 5% CO_2). Then, DMEM was removed, the formazan crystals were dissolved in DMSO (150 μL/well), and the absorbance at 570 nm was recorded. The cell viability (%) was calculated according to following equation:

$$Cell\ viability(\%) = \frac{OD_{570}(sample)}{OD_{570}(control)} \times 100$$

Where OD_{570} (sample) represents the optical density of the wells treated with various concentration of the compounds and OD_{570} (control) represents that of the wells treated with DMEM + 10% fetal calf serum (FCS). Three independent trials were conducted, and the averages and standard deviations are reported. The reported percent cell survival values are relative to untreated control cells.

Computational studies

All geometries were optimized at B3LYP level of theory and with 6-31G$_+$(d) basis set as implemented in the Gaussian 09 programs.[25] The absorption spectra were calculated using time-dependent density functional theory (TD-DFT).[26]

Acknowledgment

This work was supported by the National Natural Science Foundation of China (21271003, 21271004, 51432001 and 51472002), Science and Technology Plan of Anhui Province (1604b0602016), the Ministry of Education of the People's Republic of China, Higher Education Revitalization Plan Talent Project of Anhui Province (2013).

Notes and References

1 (a) M. C. Lindeer and M. H. Azam, Am. J. Clin. Nutr., 1996, **63**, 797-811; (b) G. Peers and N. M. Price, Natr., 2006, **441**, 341-344; (c) K. Rurack, M. Kollmannsberger and J. Daub, J Am. Chem. Soc., 2000, **122**, 968-969; (d) S. Y. Moon, N. R. Cha and Y. H. Kim, J. Org. Chem., 2004, **69**, 181-183; (e) A. Mathie, G. L. Sutton and C. E. Clarke, Pharm. Ther., 2006, **111**, 567-583.

2 (a) Y. F. Tan, N. L. Taylor and A. H. Millar, Plant Physiol., 2010, **152**, 747-761; (b) V. Desai and S. G. Kaler, Am. J. Clin. Nutr., 2008, **88**, 855-858; (c) C. N. Hancock, L. H. Stockwin and B. Han, Free Rad. Biol. Med., 2011, **50**, 110-121.

3 (a) H. I. Un, S. Wu and C. B. Huang, Chem. Commun., 2015, **51**, 3143-3146; (b) Z. Yu, R. M. Schmaltz and T. C. Bozeman, J. Am. Chem. Soc., 2013, **135**, 2883-2886; (c) Q. H. You, W. H. Chan and X. M. Zhu, Chem. Commun., 2014, **50**, 6207-6210; (d) Y. H. Lee, Y. B. Park and Y. J. Hwang, Chem. Commun., 2014, **50**, 3197-3200; (e) W. Li, X. H. Tian, B. Huang, H. J. Li, X. Y. Zhao, S. Gao, J. Zheng, X. Z. Zhang, H. P. Zhou, Y. P. Tian and J. Y. Wu, Biosensors and Bioelectronics, 2016, **77**, 530-536; (f) Z. Li, E. W. Miller, A. Pralle, E. Y. Isacoff and C. J. Chang, J. Am. Chem.Soc., 2006, 128, 10–11; (g) R. Krämer, Angew. Chem. Int. Ed., 1998, 37, 772–773.

4 (a) O. S. Bushuyev, T. A. Singleton and C. J. Barrett, Adv. Mater., 2013, **25**, 1796-1800; (b) D. Kitagawa, H. Nishi and S. Kobatake, Angew. Chem. Int. Ed., 2013, **52**, 9320-9322; (c) F. Terao, M. Morimoto and M. Irie, Angew. Chem. Int. Ed., 2012, **51**, 925-928.

5 (a) J. Kärnbratt, M. Hammarson and S. Li, Angew. Chem. Int. Ed., 2010, **49**, 1898-1901; (b) R. C. Shallcross, P. Zacharias and A. Köhnen, Adv. Mater., 2013, **25**, 469-476; (c) S. Kobatake, H. Imagawa and H. Nakatania, New J. Chem., 2009, **33**, 1362-1367.

6 (a) K. Kreger, P. Wolfer and H. Audorff, J. Am. Chem. Soc., 2010, **132**, 509-516; (b) A. Ryabchun, A. Bobrovsky and A. Sobolewska, J. Mater. Chem., 2012, **22**, 6245-6250.

7 (a) M. Han, R. Michel and B. He, Angew. Chem. Int. Ed., 2013, **52**, 1319-1323; (b) R. Tong, H. D. Hemmati and R. Langer, J. Am. Chem. Soc., 2012, **134**, 8848-8855.

8 (a) S. C. Sebai, D. Milioni and A. Walrant, Angew. Chem. Int. Ed., 2012, **51**, 2132-2135; (b) M. Lohse, K. Nowosinski and N. L. Traulsen, Chem. Commun., 2015, **51**, 9777-9780; (c) D. Kim, S. A. Lee and H. Kim, Chem. Commun., 2015, **51**, 11080-11083; (d) R. S. Stoll, M. V. Peters and A. Kuhn, J. Am. Chem. Soc., 2009, **131**, 357-367; (e) W. Fuß, C. Kosmidis and W. E. Schmid, Angew. Chem. Int. Ed., 2004, **43**, 4178-4182.

9 (a) J. C. Chan, W. H. Lam and H. L. Wong, J. Am. Chem. Soc., 2011, **133**, 12690-12705; (b) K. Liu, Y. Wen and T. Shi, Chem. Commun., 2014, **50**, 9141-9144; (c) T. Sumi, T. Kaburagi and M. Morimoto, Org. Lett., 2015, **17**, 4802-4805; (d) L. L. Hou, X. Y. Zhang and T. C. Pijper, J. Am. Chem. Soc., 2014, **136**, 910-913.

10 (a) G. Tomasello, M. J. Bearpark and M. A. Robb,. Angew. Chem., Int. Ed., 2010, **49**, 2913-2917; (b) V. I. Minkin, Chem. Rev., 2004, **104**, 2751-2776; (c) R. Klajn, Chem. Soc. Rev., 2013, **43**, 148-184; (d) Y. S. Nam, I. Yoo and O. Yarimaga, Chem. Commun., 2014, **50**, 4251-4254.

11 M. D. Yang, H. Z. Wang, J. Huang, M. Fang, B. Mie, H. P. Zhou, Y. P. Tian and J. Y. Wu, Sensors and Actuators B: Chemical, 2014, **204**, 710-715.

12 D. Maity and T. Govindaraju, Chem. Eur. J. 2011, **17**, 1410-1414.
13 S. Malkondu and S. Erdemir, Tetrahedron, 2014, **70**, 5494-5498.
14 M. Q. Wang, K. Li and J. T. Hou, Journal of Organic Chemistry, 2012, **77**, 8350-8354.
15 M. Shortreed, R. Kopelman and M. Kuhn, Analytical Chemistry, 1996, **68**, 1414-1418.
16 W. Lin, L. Yuan and Z. Cao, European Journal of Chemistry, 2009, **15**, 5096-5103.
17 (a) H. N. Kim, Z. Guo and W. Zhu, Chemical Society Reviews, 2011, **40**, 79-93; (b) N. Boens, V. Leen and W. Dehaen, Chemical Society Reviews, 2012, **41**, 1130-1172;
18 (a) H.N. Kim, Z. Guo, W. Zhu, J. Yoon and H. Tian, Chem. Soc. Rev., 2011, 40, 79–93; (b) N. Boens, V. Leen and W. Dehaen, Chem. Soc. Rev. 2012, 41, 1130–1172.
19 (a) R. Pandey, R. K. Gupta and P. Z. Li, Org. Lett., 2012, **14**, 593-595; (b) N. J. A. Coughlan, B. D. Adamson and L. Gamon, Phys. Chem. Chem. Phys., 2015, **17**, 22623-22631; (c) X. Li, L. W. Chung and K. J. Morokuma, J. Chem. Theory Comput, 2011, **7**, 2694-2698.
20 T. Sarkar, S. Banerjee and A. Hussain, RSC Advances, 2015, **5**, 16641.
21 W. Li, Y. Zhang, X. P. Gan, M. D. Yang, B. Mie, M. Fang, Q. Y. Zhang, J. H. Yu, J. Y. Wu, Y. P. Tian and H. P. Zhou, Sensors and Actuators B: Chemical, 2015, **206**, 640-646.
22 W. Lin, L. Yuan, Z. Cao, Y. Feng and L. Long, Eur. J. Chem., 2009, **15**, 5096–5103.
23 A. Rai, N. Kumari, R. Nair, K. Singh and L. Mishra, RSC Adv., 2015, **5**, 14382.
24 T. Mosmann, J. Immunol. Methods, 1983, **65**, 55-63
25 (a) M. J. Frisch, G. W. Trucks, H. B. Schlegel, G. E. Scuseria, M. A. Robb, J. R. Cheeseman, G. Scalmani, V. Barone, B. Mennucci and G. A. Petersson, Wallingford, CT, 2009; (b) A. D. Becke, J. Chem. Phys. 1993, **98**, 5648-52.
26 (a) R. Bauernschmitt and R. Ahlrichs, Chem. Phys. Lett., 1996, **256**, 454-464; (b) R. E. Stratmann, G. E. Scuseria and M. J. Frisch, J. Chem. Phys., 1998, **109**, 8218-8224.

Graphical Abstract

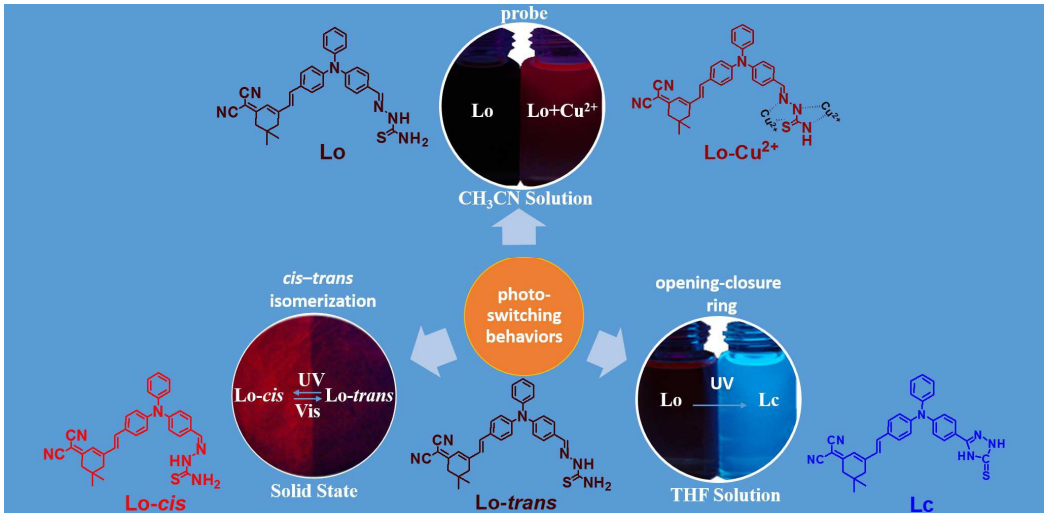

Two independently addressable photochromic systems based on the distinct mechanisms and selective recognition for Cu^{2+} were investigated in detail.